Laser chaos induced by delayed-feedback and external modulation

C. Juang[1], S. M. Chang[2], N. K. Hu[3], C. Lee[3], and W. W. Lin[2]

[1]Electronics Dept., Ming Hsin University, Hsinfeng, Hsinchu, Taiwan, R.O.C.

[2]Dept. of Math., National Tsing Hua University, Hsinchu, Taiwan, R.O.C.

[3]Teh-Fa Tech., Hsitz, Taipei, Taiwan, R.O.C.

Electronic-controlled routes to chaos in a quantum-well laser diode are carried out by a delayed-feedback technique. By introducing an extra delayed-feedback control term $cS_n(t-\tau)$, chaotic light output can be achieved at relatively low bias and small modulation depth. The interaction between external modulation and delay forms quasi-2 period routes to chaos by varying modulation amplitude b and intermittency routes to chaos by varying modulation frequency f_o. Numerical analysis and experimental results agree qualitatively.

KEYWORDS: Quasi-2 period routes to chaos, Intermittency routes to chaos, Quantum-well laser diodes, Delayed-feedback.

1. Introduction

Dynamical chaos in laser diodes has drawn much interest due to its potential application in private communication[1]. There are many ways to generate chaotic light output from a laser diode. In general, one can catalog these techniques as optical approach and electronic approach. In optical approach, Fischer et at., have achieved high-dimensional chaos using an external cavity[2]. Annovazzi-Lodi et at., have reported chaotic behaviors by an optical injection from a second laser diode[3]. In electronic approach, a laser diode is injected by a sinusoidal and a bias current $I = a + b \sin 2\pi f_o t$, where a is the bias current, b is the modulation current, f_o is the external modulation frequency[4,5]. In general, high bias and strong current modulation, or two tone modulation are required to achieve chaos.

Delayed-feedback is known to have rich properties in nonlinear dynamics of laser diodes[6]. This delay technique has also been combined with optical injection to achieve stability in a laser diode[7]. In this work, electronic injection is incorporated with a delayed-feedback to achieve chaos in a laser diode. The overall current injected into the laser diode then is given by

$$I = a + b \sin 2\pi f_o t + cS_n(t - \tau), \tag{1}$$

where c is the current gain, and τ is the loop delay time. With the introduction of the extra delay term $cS_n(t-\tau)$, it is shown that the chaotic light output can obtained at relatively low bias and small modulation depth. Note that without modulation and delay, the system always converges to a fixed point. The interaction between external modulation and delay forms quasi-2 period routes to chaos by varying b

and intermittency routes to chaos by varying f_o. Section 2 formulates a laser diode with a delayed-feedback. Bifurcation diagrams versus b and f_o are shown. Section 3 presents the experimental results to verify quasi-2 period routes to chaos and intermittency routes to chaos.

2. Numerical Analysis

a. Delay differential rate equation

The three-dimensional quantum well rate equation to describe the dynamics of carrier in separate confinement regions I_s, in quantum well region I_n, and photon density S_n is given by[8]

$$\begin{aligned}
\tau_s \frac{dI_s}{dt} &= I - (1 + \frac{\tau_s}{\tau_n})I_s, \\
\tau_n \frac{dI_n}{dt} &= I_s - I_n - G(1 - \epsilon_n S_n)S_n, \\
\frac{C_p}{\Gamma}\frac{dS_n}{dt} &= G(1 - \epsilon_n S_n)S_n + \beta I_n - \frac{S_n}{\Gamma R_p},
\end{aligned} \tag{2}$$

where τ_s is the carrier transport time across separate confinement heterostructure regions, τ_n is the bimolecular recombination lifetime, Γ is the optical confinement factor per well, β is the spontaneous emission factor, and ϵ is the gain compression factor. In addition, the optical gain function is expressed by a square dependence on the recombination current J_{nom}, $G = D(J_{nom} - 2 \times 10^{13})^2$, where D is a constant, $J_{nom} = I_n/V_a$, and V_a is the active layers volume. Table I lists all the parameters of the QW laser diode used in the simulation. Without feedback and modulation ($b = c = 0$), L-I curve simulation suggests a threshold current I_{th} of 38 mA. This agrees with a simple steady state analysis, in which the threshold current can be

approximated as $(1+\tau_s/\tau_n)(V_aN_0+V_a/\sqrt{\Gamma R_p D})$. The step-response simulation (switching from 0 to a, where $a=1.5I_{th}$) results in a relaxation oscillation period T_r of 1.5 nsec.

To solve the delay differential equations, Eq. 2 can be expressed as $\dot{\mathcal{X}} = \mathcal{F}(t,\mathcal{X}) + A\mathcal{X}(t-\tau)$, where $\mathcal{X} \in R^3$ is the state variable $\mathcal{X} = (X^1, X^2, X^3) = (I_s, I_n, S_n)$, $\mathcal{F} = R \times R^3 \to R^3$ is a nonlinear function, and $A \in M^{3\times 3}$ is a matrix with a nonzero term. By modifying the fourth-order Runge-Kutta-Fehlberg method (RKF45)[9] for a fixed time-step $\Lambda(=\tau/n)$, we have

$$\begin{aligned} \mathcal{X}_m &= \varphi(\mathcal{X}_{m-1}, \mathcal{X}_{m-n}), \\ &= \mathcal{X}_{m-1} + \sum_{i=0}^{5} c_i F_i^m, \end{aligned} \tag{3}$$

where

$$\begin{aligned} F_0^m &= \mathcal{F}(m\Lambda, \mathcal{X}_{m-1}) + A\mathcal{X}_{m-n}, \\ F_i^m &= \mathcal{F}(m\Lambda + q_i, \mathcal{X}_{m-1} + \sum_{j=0}^{i-1} h_{ij} F_j^m) + A[\frac{\Lambda - q_i}{\Lambda}\mathcal{X}_{m-n} + \frac{q_i}{\Lambda}\mathcal{X}_{m-n+1}], \end{aligned} \tag{4}$$

and m is the time-step index ($m \geq n$), and c_i, q_i and h_{ij} are the coefficients of the RKF45.

b. Delay loop frequency f_d

By solving Eq. 2 with (b=0), one can obtain the delay loop frequency from the Fourier transform of the S_n. Figure 1 shows the delay loop frequency f_d versus delay time τ when $a=1.5I_{th}$. With delay time alone, periodical solutions of the S_n are observed in this model. The natural frequency of the system will not compete

with the delay loop frequency because the oscillation will not sustain long enough. However, it dose affect the loop delay frequency. As shown in the Figure, f_d repeated itself in a period of 1.5 nsec, which is close to the relaxation oscillation period at $a = 1.5I_{th}$.

c. Quasi-2 routes to chaos by varying b

Quasi-periodicity involves competition between two independent frequencies characterizing the dynamics of the system. As these two frequencies compete with each other nonlinearly, the result can then be chaos. In general, there seems to be a complex interplay between the strength of the coupling and the amplitude of each frequency. In our system, the first frequency is the delay loop frequency, and the second competing independent frequency is the external modulation frequency f_o. Ony the amplitude of the second frequency is easily adjustable. Thus, Fig. 2 shows the bifurcation diagram with S_n versus b in I_{th} when $a = 1.5I_{th}$, $\tau = 8$ nsec, $c = 0.035$, and $f_o = 1.33f_d$. Note that the frequency ratio must be irrational. In the three-dimensional phase diagram (I_s, I_n, and S_n) of the rate equations, let Σ be a two-dimensional hyper plane through a point (0.05, 0.0377, 0.4) with normal direction [0, 1, 0]. If the trajectory in the phase diagram mapped on the hyper plane densely fills out closed curve, then the solution forms a quasi-2 periodic orbit. When $b = 0$, the system starts with a fixed point attractor. As a control parameter is changed $b \in (0, 3.5)$, the system undergoes a bifurcation to develop into a quasi-2 period attractor. The second frequency may appear further change in the control parameter. When b is increased to 0.45, the quasi-periodicity route to chaos sets in.

Figures 3a and 3b show Poincaré maps at b=0.2 and b=0.45 when $a = 1.5I_{th}$, $\tau = 8$ nsec, $c = 0.035$, and $f_o = 1.33f_d$. When b=0, the system has an asymptotically stable fixed point. As b increases to 0.2, the fixed point expands into an invariant closed-loop circle, a set like a circle which captures the point of a solution sequence. When b=0.45, the circle breaks up into a complicated attracting set. These behaviors characterize the quasi-period and chaos in the system.

d. Intermittency routes to chaos by varying f_o

Intermittency occurs when the behavior of the system switches back and forth intermittently between periodic and chaotic behaviors. Figure 4 shows the bifurcation diagram with S_n versus f_o when $a = 1.5I_{th}$, $\tau = 8$ nsec, $c = 0.035$, and $b = 0.45I_{th}$. As shown, the behavior appear to have certain character (e.g., periodic) for some times and then abruptly switches to behaviors of a qualitatively different character (e.g., chaotic). The switching between these two behaviors seems to be random. In fact, since $b = 0.45I_{th}$ one would expect chaotic behaviors all the way. However, intermittency behavior is chaotic behavior characterized by irregularly occurring episodes of periodic behavior. The cause of the periodic behavior is a trapping of trajectories in the gap regions. At the bifurcation event, the limit cycle associated with the two competing frequencies become unstable. The bursts of two-frequency behavior mixed with intervals of chaotic behavior is seen. This effect previously described as "Hopf-bifurcation intermittency" can be found in some other systems (see Ref. [10], for example). In addition, as the control parameter value is changed, the time spend being chaotic increases and time being periodic decreases.

See the gap is getting smaller.

3. Experimental Results

a. Experimental setup

The schematic of the experimental setup is shown in the Fig. 5. The light source is a 1.55 μm InGaAsP laser diode (SDO Comm.) with a threshold of 13 mA. The total driving current is given by Eq. 1. $a + b \sin 2\pi f_o t$ is provided by a signal generator and a laser driver. A splitter is inserted in the loop. Part of the light is directed into a power spectrum analyzer. Part of the light is used to establish a delay loop. Delay is achieved by optical fiber delay line at various lengths from 0.3 meter to 1 meter, which is estimated to correspond to a delay time of 3 to 10 nsec. A optical fiber delay line, a high speed InGaAs receiver (EO Tech.), and a 30 dB wide-band amplifier (Amplifier Research) complete a delay feedback loop and an adjustable gain. The delay signal $cS_n(t-\tau)$ is then injected into the laser diode along with the external modulation and DC bias current. Frequency spectra of the total light output extracted from a splitter are then shown on a power spectrum analyzer (Advantest).

b. Quasi-2 routes to chaos by varying b

By adjusting the power level of the external modulation, one can investigate the quasi-routes to chaos. Figures 6a, 6b, 6c, and 6d show the measured power spectra for various experimental situations: (a) f_d=50Mhz, period-one, (b) f_d=50Mhz, P_o = -20dbm, f_o = 87.6Mhz, period-two, (c) f_d=50Mhz, P_o = 1.4dbm,

$f_o = 87.6$Mhz, quasi-state, and (d) f_d=50Mhz, $P_o = 5.9$dbm, f_o =87.6Mhz, chaotic state. For (a), no external modulation is injected as such a single delay loop frequency is presented, as expected. By adding a small power of second frequency f_o (b), the system shows independent oscillation. As the power level of the second frequency increases, the system undergoes a bifurcation to develop into a quasi-2 period attractor. Note that for the quasi-periodic case, all the peaks are a linear combination of $f_o + f_d$ and their subharmonics. Since their amplitudes decreases with increasing coefficients, peaks at frequencies corresponding to large values of the coefficients, are eventually below the overall noise level of the experiments. In the chaotic case (d), peaks at two basic frequencies are presented , but that spectrum has also developed a broad continuous component. The broad continuous component is above the noise level, as evident in Fig. 6c. Also, the situation in Fig. 6d is in contrast to that on Fig. 6c, where the only apparent frequency components are discrete. The presence of a continuous component in a frequency power spectrum indicates chaotic oscillations in the laser diode. Therefore, quasi-2 period routes to chaos can then be established, which is qualitatively agree with previous numerical analysis.

c. Intermittency routes to chaos by varying f_o

By scanning through the external modulation frequency, one can further investigate the intermittency routes to chaos. Figures 7a, 7b, 7c, and 7d show the measured power spectra for various experimental situations: (a) f_d=61.7Mhz, P_o = 10dbm, f_o = 79.6Mhz, period-two, (b) f_d=61.7Mhz, P_o = 10dbm, f_o = 84.1Mhz,

chaotic state, (c) f_d=61.7Mhz, P_o = 10dbm, f_o = 123.5Mhz, period-two, and (d) f_d=61.7Mhz, P_o = 10dbm, f_o = 162.3Mhz, chaotic state. Intermittency signifies an episodic switching between different types of behaviors. In the intermittency transition, one has a simple periodic orbit which is replaced by chaos as the control parameter passes through a critical transition value. This switching occurs seemingly random times as follows: chaos → periodic → chaos → periodic → chaos→ and so on. The measured power spectra indicates (1) abrupt switching (see (a) → (b) in a small change in external frequency), and (2) random and repeating switching ((a) → (b) → (c) → (d)). Therefore, intermittency routes to chaos can be established, which is also qualitatively agree well with previous numerical analysis.

4. Conclusions

In conclusion, a delayed-feedback technique is used to achieve routes to chaos in a quantum-well laser diodes at relatively low bias and small modulation depth. In theory, quasi-periodicity routes to chaos and intermittency routes to chaos can be visualized by the bifurcation diagram and Poincaré map for solving the delay differential rate equation. In experiment, power spectra also indicate quasi-2 period routes to chaos by varying modulation amplitude b and Hopf-bifurcation intermittency routes to chaos by varying modulation frequency f_o. This study set up a controllable way to achieve chaotic laser for the future study in the synchronization between two delayed chaotic lasers, and in the realization of the optical chaotic communication.

Table I. The parameters used for the simulation of quantum well lasers.

parameters	value	unit
τ_s	6	ps
τ_n	22.5	ns
ϵ	10^{-17}	cm^3
Γ	0.2	-
R_p	59.5	Ω
C_p	0.0489	pf
β	10^{-4}	-
D	1.79×10^{-29}	$\mathrm{V}^{-1}\mathrm{A}^{-1}\mathrm{m}^6$
qV_a	6.85×10^{-35}	$\mathrm{m}^3\mathrm{C}$

References:

(1) C. R. Mirasso, P. Colet, and P. Garcia-Fernandez: IEEE J. Quantum Electron. **8** 1996 299.

(2) I. Fischer, O. Hess, W. Elsäβer, and Göbel: Phy. Rev. Lett. **73** 1994 2188.

(3) V. Annovazzi-Lodi, S. Donati, and A. Scire: IEEE J. Quantum Electron. **33** 1997 1537.

(4) S. Bennett, C. M. Snowden, and S. Iezekiel: IEEE J. Quantum Electron. **33** 1997 2076.

(5) E. Hemery, L. Chusseau, and J. M. Lourtioz: IEEE J. Quantum Electron. **26** 1990 633.

(6) F. Y. Lin and J. M. Liu: IEEE J. Quantum Electron. **39** 2003 562.

(7) P. Saboureau, J. P. Foing, and P. Schanne: IEEE J. Quantum Electron. **33** 1997 1582.

(8) C. Juang, C. C. Huang, T. M. Hwang, J. Juang, and W. W. Lin: Optics comm., **192** 2001 77.

(9) D. Kincaid and W. Cheney: Numerical Analysis/Pacific Grove 1991.

(10) J. Y. Huang and J. J. Kim: Phys. Rev. **A36** 1987 1495.

Figure Captions:

Fig. 1. Delay loop frequency f_d versus delay time τ when $a = 1.5I_{th}$.

Fig. 2. Bifurcation diagram with S_n versus b in I_{th} when $a = 1.5I_{th}$, $\tau = 8$ nsec, $c = 0.035$, and $f_o = 1.33f_d$.

Figs. 3a and 3b. Poincaré maps at b=0.2 and b=0.45 I_{th} when $a = 1.5I_{th}$, $\tau = 8$ nsec, $c = 0.035$, and $f_o = 1.33f_d$.

Fig. 4. Bifurcation diagram with S_n versus f_o when $a = 1.5I_{th}$, $\tau = 8$ nsec, $c = 0.035$, and $b = 0.45I_{th}$.

Fig. 5. Experimental setup of a laser diode using delay-time feedback control.

Figs. 6a, 6b, 6c, and 6d. Measured power spectra for various experimental situations: (a) f_d=50Mhz, period-one, (b) f_d=50Mhz, P_o = -20dbm, f_o = 87.6Mhz, period-two, (c) f_d=50Mhz, P_o = 1.4dbm, f_o = 87.6Mhz, quasi-state, and (d) f_d=50Mhz, P_o = 5.9dbm, f_o = 87.6Mhz, chaotic state.

Figs. 7a, 7b, 7c, and 7d. Measured power spectra for various experimental situations: (a) f_d=61.7Mhz, P_o = 10dbm, f_o = 79.6Mhz, period-two, (b) f_d=61.7Mhz, P_o = 10dbm, f_o = 84.1Mhz, chaotic state, (c) f_d=61.7Mhz, P_o = 10dbm, f_o = 123.5Mhz, period-two, and (d) f_d=61.7Mhz, P_o = 10dbm, f_o = 162.3Mhz, chaotic state.

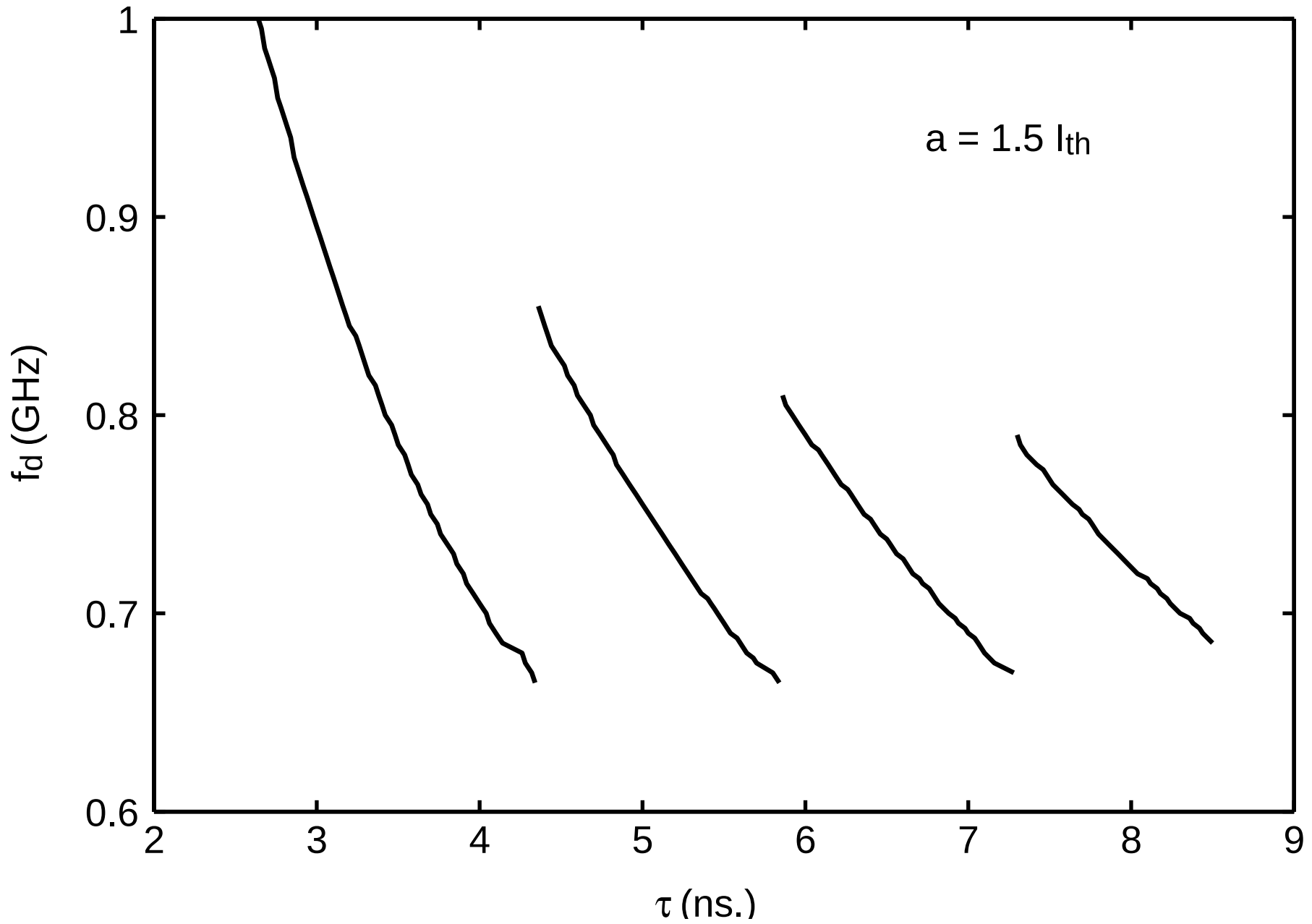
a = 1.5 I_{th}
1
0.9
0.8
0.7
0.6
f_d (GHz)
2
3
4
5
6
7
8
9
τ (ns.)

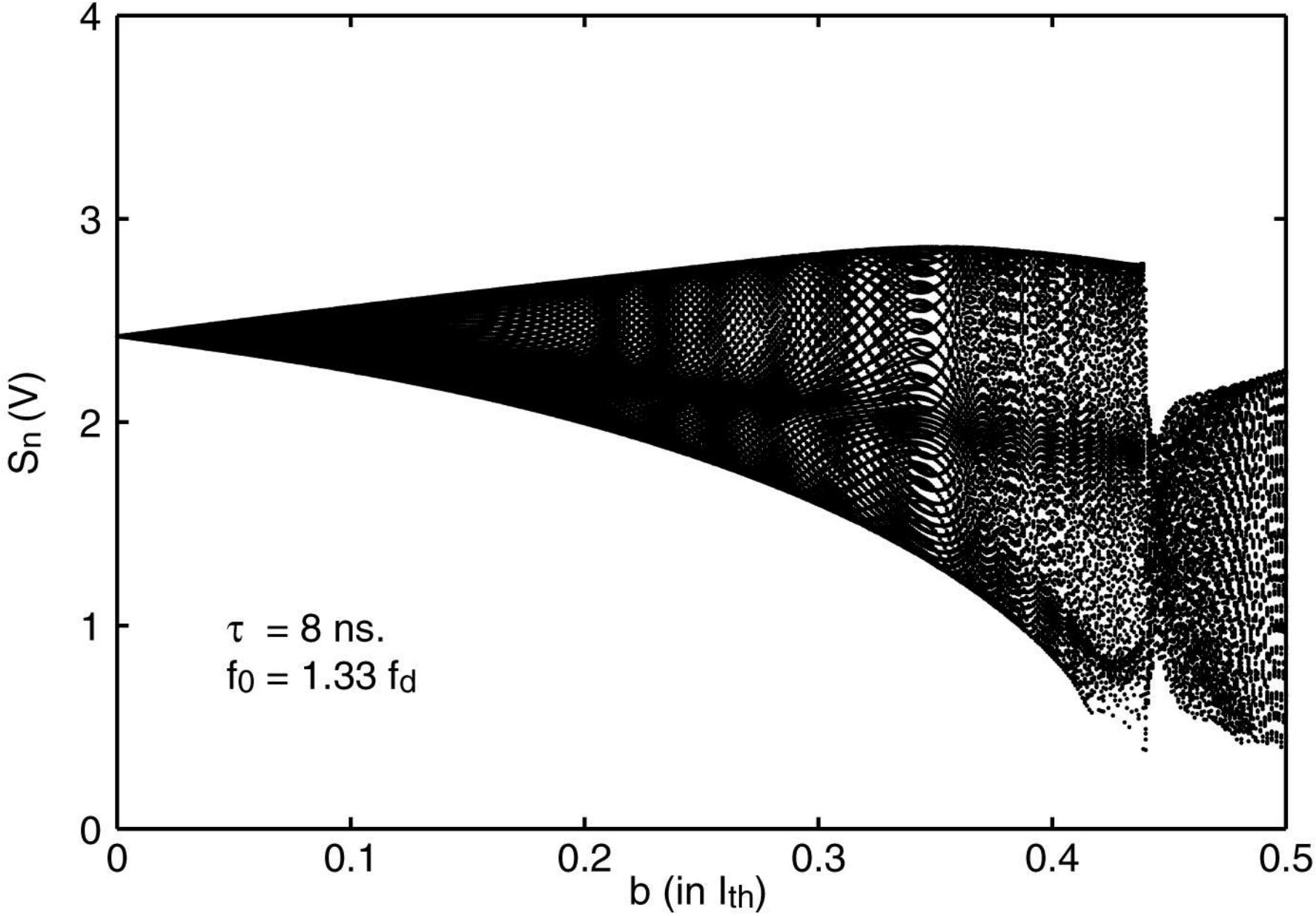
4
3
2
1
0
S_n (V)
0
0.1
0.2
0.3
0.4
0.5
b (in I_{th})
τ = 8 ns.
f_0 = 1.33 f_d

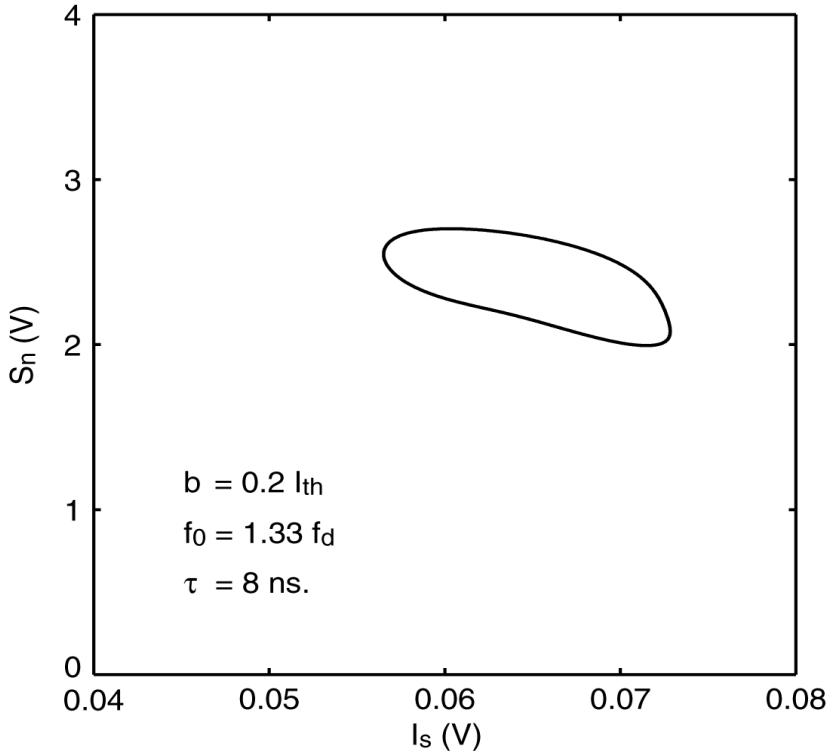
4
3
2
1
0
S_n (V)
b = 0.2 I_{th}
f_0 = 1.33 f_d
τ = 8 ns.
0.04
0.05
0.06
0.07
0.08
I_s (V)

(a)

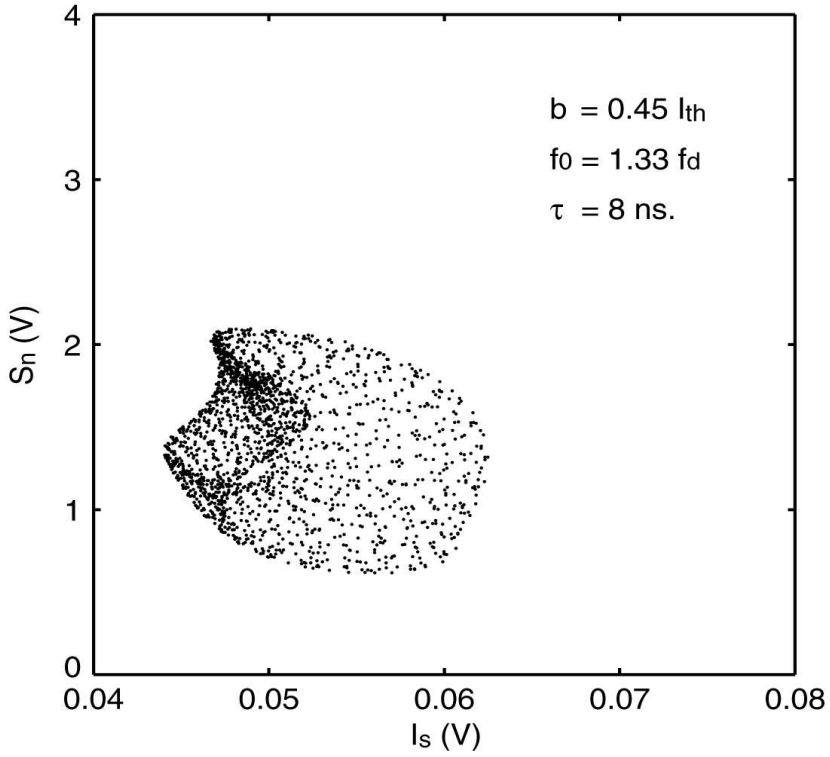
4
3
2
1
0
S_n (V)
b = 0.45 I_{th}
f_0 = 1.33 f_d
τ = 8 ns.
0.04
0.05
0.06
0.07
0.08
I_s (V)

(b)

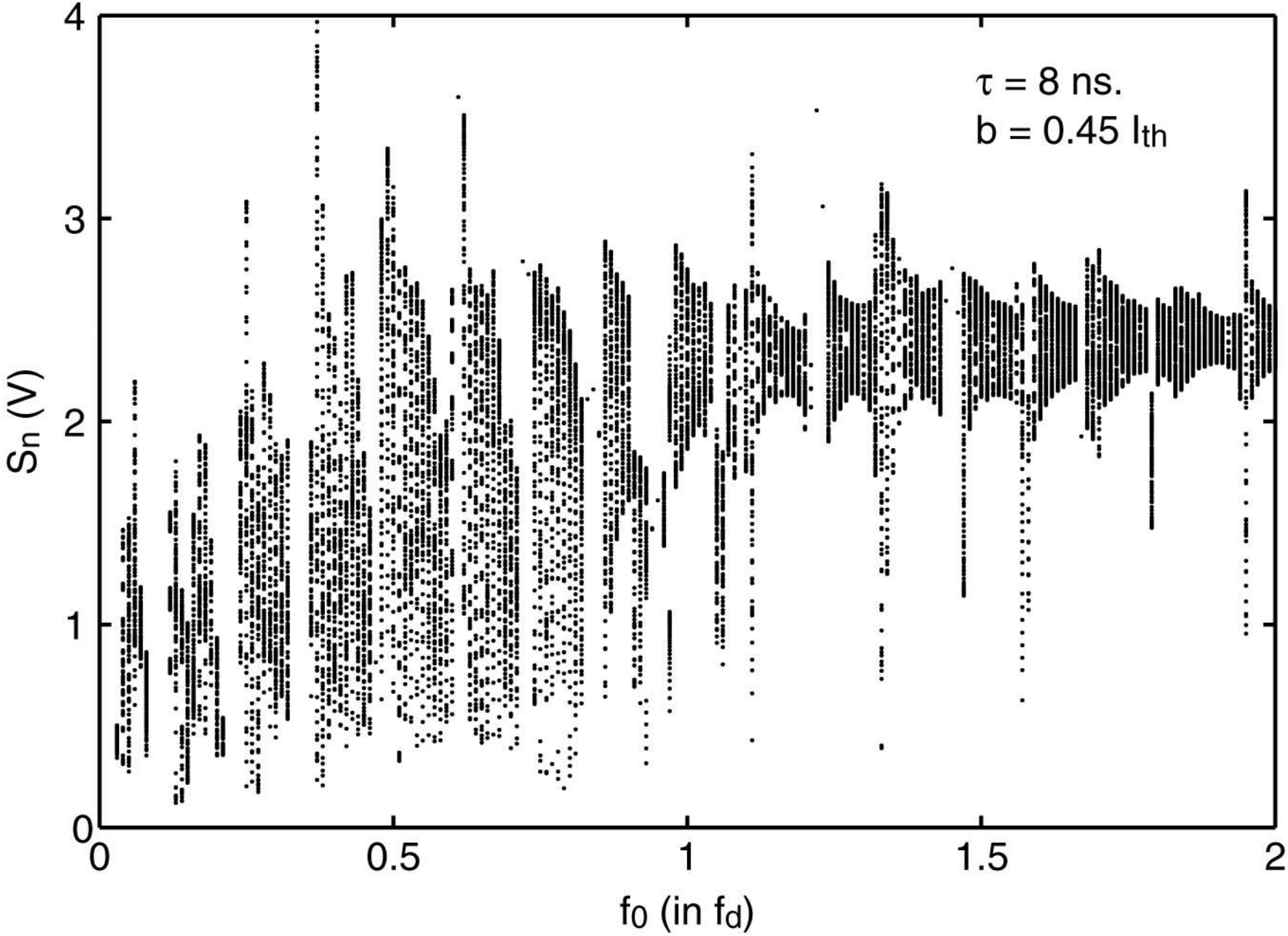
τ = 8 ns.
b = 0.45 I_th
S_n (V)
f_0 (in f_d)
0
1
2
3
4
0
0.5
1
1.5
2

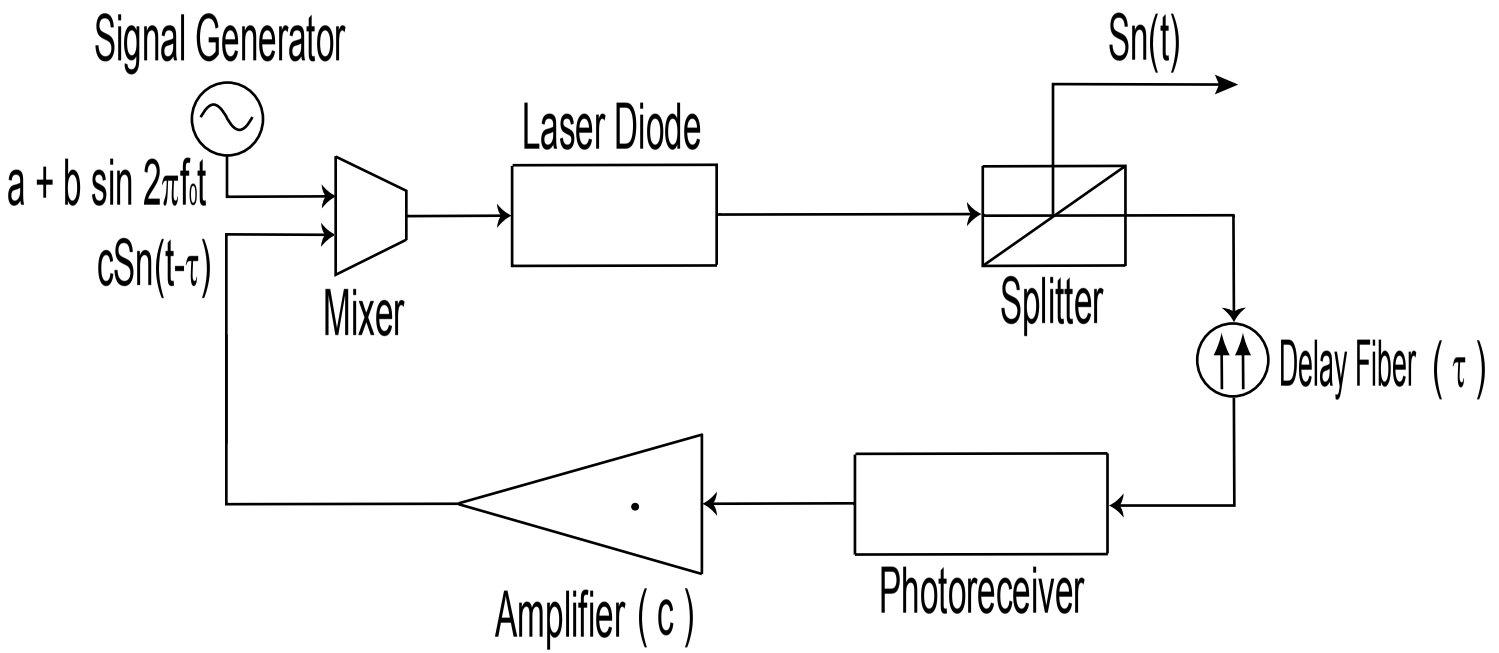
Signal Generator
a + b sin 2πf₀t
cSn(t-τ)
Mixer
Laser Diode
Sn(t)
Splitter
Delay Fiber (τ)
Photoreceiver
Amplifier (c)

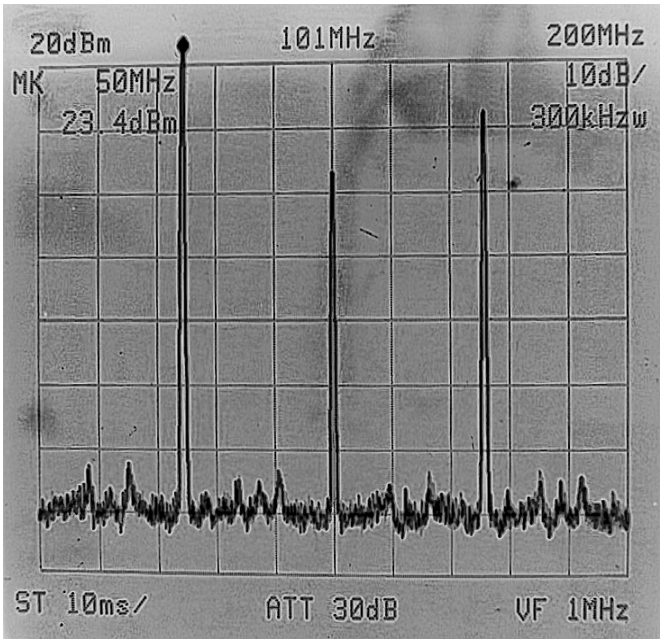
20dBm
101MHz
200MHz
MK 50MHz
10dB/
23.4dBm
300kHzw
ST 10ms/
ATT 30dB
VF 1MHz

(a)

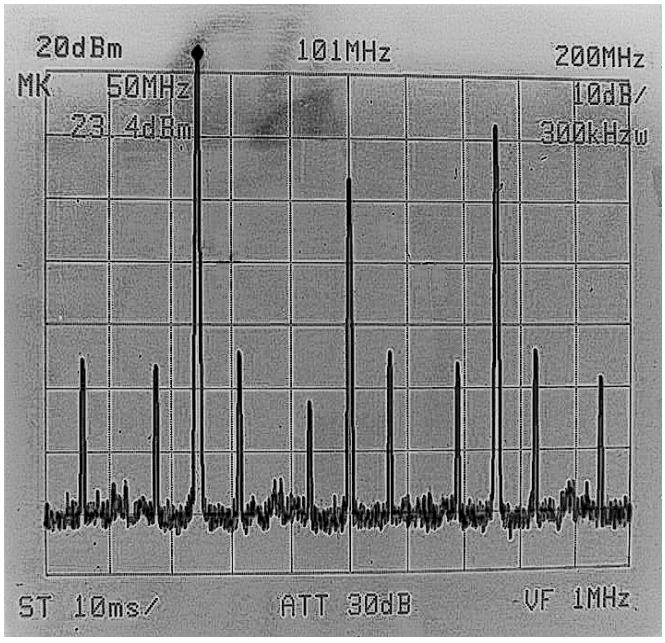
20dBm
101MHz
200MHz
MK 50MHz
10dB/
23.4dBm
300kHzw
ST 10ms/
ATT 30dB
VF 1MHz

(b)

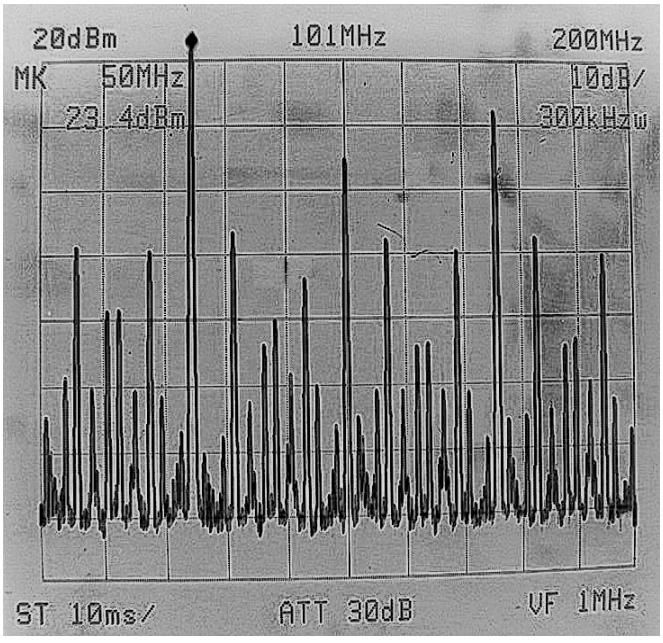
20dBm
101MHz
200MHz
MK 50MHz
10dB/
23.4dBm
300kHzw
ST 10ms/
ATT 30dB
VF 1MHz

(c)

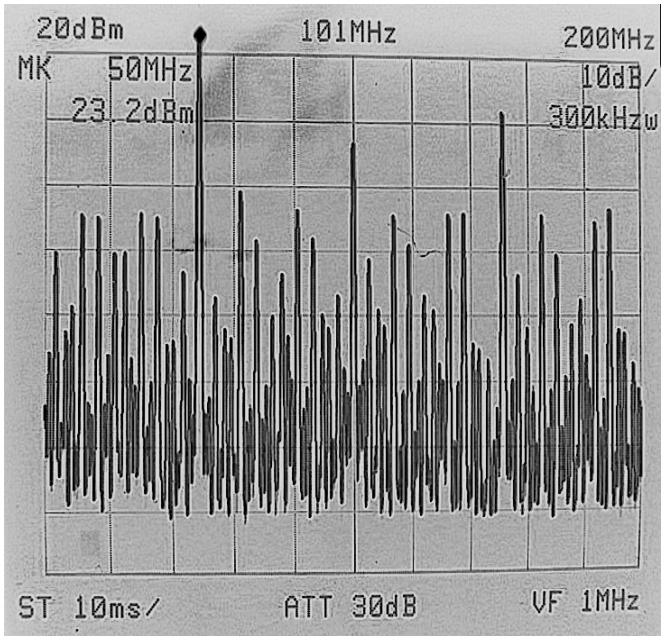
20dBm
101MHz
200MHz
MK 50MHz
10dB/
23.2dBm
300kHzw
ST 10ms/
ATT 30dB
VF 1MHz

(d)

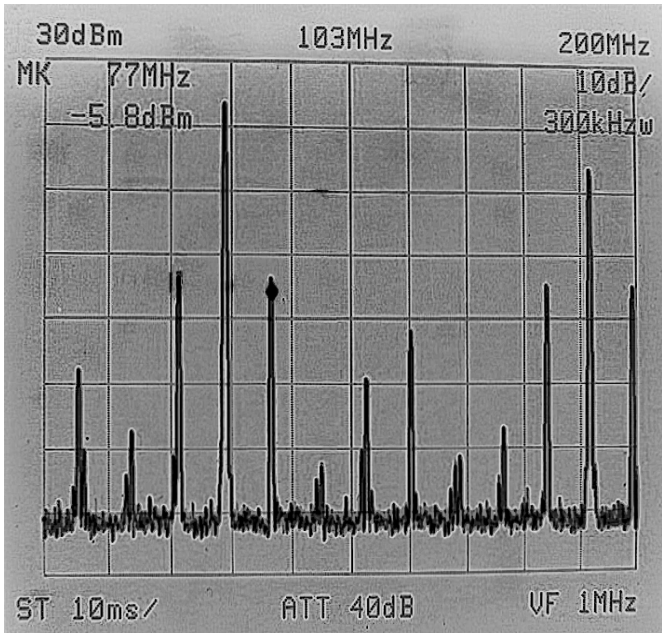
30dBm
103MHz
200MHz
MK 77MHz
-5.8dBm
10dB/
300kHzw
ST 10ms/
ATT 40dB
VF 1MHz

(a)

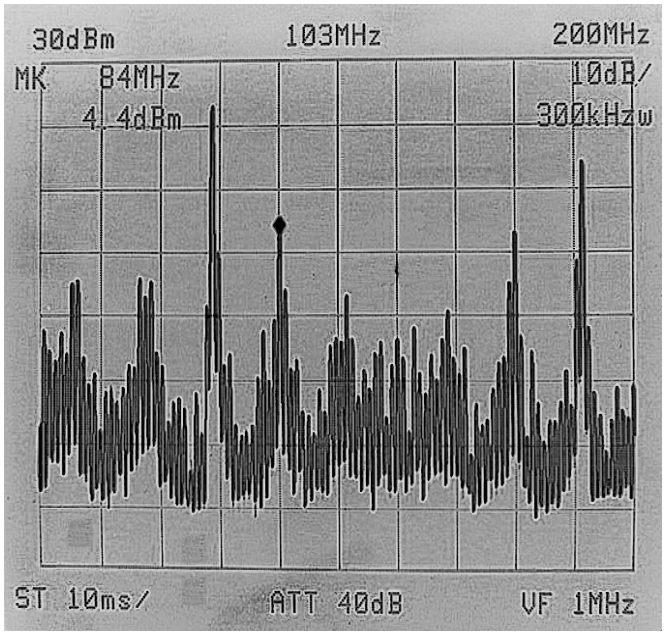
30dBm
103MHz
200MHz
MK 84MHz
4.4dBm
10dB/
300kHzw
ST 10ms/
ATT 40dB
VF 1MHz

(b)

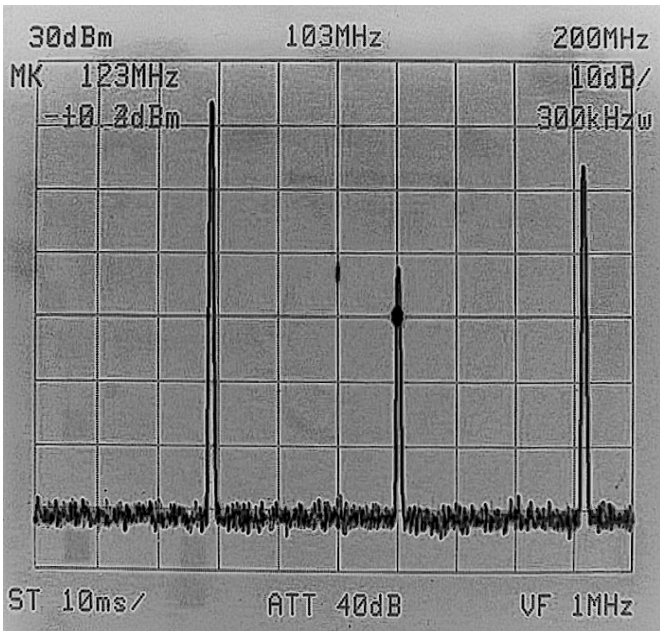
30dBm
103MHz
200MHz
MK 123MHz
-10.2dBm
10dB/
300kHzw
ST 10ms/
ATT 40dB
VF 1MHz

(c)

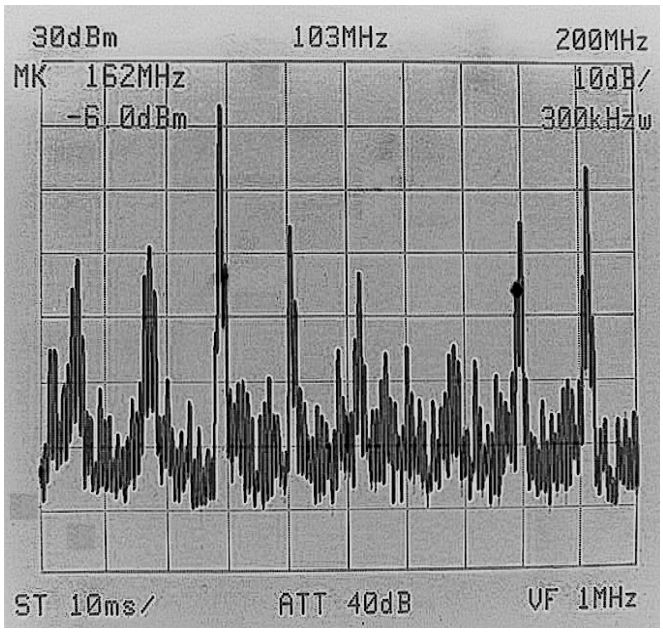
30dBm
103MHz
200MHz
MK 162MHz
-6.0dBm
10dB/
300kHzw
ST 10ms/
ATT 40dB
VF 1MHz

(d)